Wetlands Ecology and Management **10:** 85–96, 2002.

Monitoring the recovery of *Juncus roemerianus* marsh burns with the normalized difference vegetation index and Landsat Thematic Mapper data

Elijah W. Ramsey III*, Sijan K. Sapkota[1], Frank G. Barnes[2] & Gene A. Nelson
*U.S. Geological Survey, National Wetlands Research Center; [1]Johnson Controls World Services Inc.; [2]Oak Ridge Associated Universities; 700 Cajundome Blvd., Lafayette, LA 70506, U.S.A.; *Author for correspondence: Tel: (337)266-8575, Fax: (337)266-8616, E-mail: elijah_ramsey@usgs.gov*

Received 15 May 2000; accepted in revised form 1 January 2001

Key words: Juncus roemerianus, Landsat TM, marsh burn, monitoring, NDVI, recovery, vegetation indices

Abstract

Nine atmospherically corrected Landsat Thematic Mapper images were used to generate mean normalized difference vegetation indices (NDVI) at 11 burn sites throughout a coastal *Juncus roemerianus* marsh in St. Marks National Wildlife Refuge, Florida. Time-since-burn, the time lapse from the date of burn to the date of image collection, was related to variation in mean NDVI over time. Regression analysis showed that NDVI increased for about 300 to 400 days immediately after the burn, overshooting the typical mean NDVI of a nonburned marsh. For about another 500 to 600 days NDVI decreased until reaching a nearly constant NDVI of about 0.40. During the phase of increasing NDVI the ability to predict time-since-burn was within about ±60 days. Within the decreasing phase this dropped to about ±88 days.

Examination of each burn site revealed some nonburn related influences on NDVI (e.g., seasonality). Normalization of burn NDVI by site-specific nonburn control NDVI eliminated most influences. However, differential responses at the site-specific level remained related to either storm impacts or secondary burning. At these sites, collateral data helped clarify the abnormal changes in NDVI. Accounting for these abnormalities, site-specific burn recovery trends could be broadly standardized into four general phases: Phase 1 – preburn, Phase 2 – initial recovery (increasing NDVI), Phase 3 – late recovery (decreasing NDVI), and Phase 4 – final coalescence (unchanging NDVI). Phase 2 tended to last about 300 to 500 days, Phase 3 an additional 500 to 600 days, and finally reaching Phase 4, 900 to 1,000 days after burn.

Introduction

Grassland fires are a major component of burns occurring from open prairie to coastal wetlands (Johnson and Knapp, 1993). Prairie grass response to fire has been documented, but little information exists concerning the effect of fire on wetland marsh (Johnson and Knapp, 1993; Taylor et al., 1994). This information would provide ecologists with improved inputs to ecological models used to understand the effects of fires. In turn, model results could provide resource managers a rational decision-making system for evaluating fire management strategies.

Direct assessment techniques can be used to monitor local effects, but surveys to assess the spatial and temporal variability of burns are constrained by time, personnel, and costs. Further, the long-term effects of burns within a regional context are poorly known and understood. To help alleviate these limitations, our research explored the uses of remote sensing to monitor marsh burn recovery. Remote sensing offers the advantage of repetitive coverage (or temporal monitoring) of large regions. The challenge is to transform the temporal patterns revealed in the remote sensing data into quantitative determinations of the rates of development of marsh resources, and

into qualitative judgments of external effects on these resources (Lulla and Mausel, 1983). In addition, to be effective for operational management, the procedures used to transform the remote sensing data into products useful to the resource manager must be cost effective, in a form readily implemented in available image processing software, and verified and calibrated with current operational ground-based measurements (Teuber, 1990).

In this study, our objective was to link the burn recovery of *Juncus roemerianus* (commonly known as black needlerush) to changes in Landsat Thematic Mapper (TM) data. Since 1983, the TM sensor has been providing relatively inexpensive regional data every 16 days at a moderately high spatial resolution (about 30 m by 30 m), although, cloud contamination can severely limit the number of useable collections. Landsat 5 Thematic Mapper (TM) data covers an area about 185 km by 185 km at a cost of about 0.014 to 0.018 cents (U.S.) per hectare (government rate). Data handling and analyses can be performed on a standard computer platform with widely available image processing software.

The choice of *J. roemerianus* is important to coastal resource management because it is not only common along the U.S. east coast, but also it dominates the landscape and makes up the majority of biomass in marshes of the U.S. northeast Gulf Coast (Stout, 1984). The study took place in the St. Marks National Wildlife Refuge (NWR), Florida (Figure 1) near the center of *J. roemerianus* dominance in the northeast Gulf Coast. Although *J. roemerianus* growth patterns have been documented in various site specific studies including St. Marks NWR (Hopkinson et al., 1978; Kruczynski et al., 1978; Johnson and Knapp, 1993; Ramsey et al., 1998), no study linking the growth pattern to remote sensing data has been performed.

Site-specific observations of *J. roemerianus* burn recovery showed that following a relatively intense burn, a burn site progresses from grass stubble to short, mostly vertical shoots, to a mature canopy of a fairly vertical lower canopy and an upper canopy of mixed orientations. During the regrowth, the density of the canopy increases, and the upper canopy gains a higher density than the lower canopy (Ramsey et al., 1999). Height measurements of mature canopies (nonburned for at least 5 years) ranged from 80 cm to around 120 cm. We obtained biomass ranging from 580 to 1,070 gm/m^2 in these burn sites, similar to Kruczynski et al.'s (1978) mean total biomass of 600 gm/m^2 in high marsh and 1,063 gm/m^2 in upper (middle) marsh. In essence, as the site progressed from new burn to mature canopy, the grass canopy changed from nearly vertical, low density new green shoots (around 100%) to a mixed orientation, medium to high density combination of dead and live shoots (around a 50/50 mix).

Except for sites recovering from recent burns (< 2 to 3 months), canopies usually contain a high proportion of dead material (Hopkinson et al., 1978; Ramsey et al. – unpublished data). Live and dead biomass proportions in mature *J. roemerianus* marshes have been reported to be relatively constant without clear seasonal trends (Williams and Murdoch, 1972); growth, mortality, and disappearance of dead materials occur continuously throughout the year (Hopkinson et al., 1978). Field observations and analysis of radar data indicate that recovery of *J. roemerianus* from burning can require up 3 years (Hopkinson et al., 1978; Ramsey et al., 1992, 1999). A few months after burning, the *J. roemerianus* marsh begins a slow recovery that is depicted by a constant and nearly equal addition of live and dead material. After reaching maturity, a *J. roemerianus* marsh turnover rates of both live and dead biomass remain nearly constant showing no clear seasonal pattern.

Methods

Nine late winter and late summer TM images were acquired of the St. Marks NWR between 1990 and 1994, that included 18 September 1990, 9 February 1991, 20 August 1991, 28 February 1992, 6 August 1992, 18 March 1993, 25 August 1993, 5 March 1994, and 13 September 1994. Selection was severely limited because of the prevalence of clouds during all seasons. Popcorn clouds contaminated even the August 1992 image, making it necessary to slightly adjust the placement or extent of some burn and control sites in this image to account for clouds and cloud shadows. To perform the multidate analysis, all images were registered to a geometrically rectified 1990 TM image (25 m by 25 m spatial resolution). To more precisely identify burn extent, coregistered aerial color infrared photography (CIR, ±3 m spatial resolution) collected in 1988 and 1992 was added to the image database. Root-mean-square error values and visual examination suggested a registration accuracy of ±1 pixel for all images.

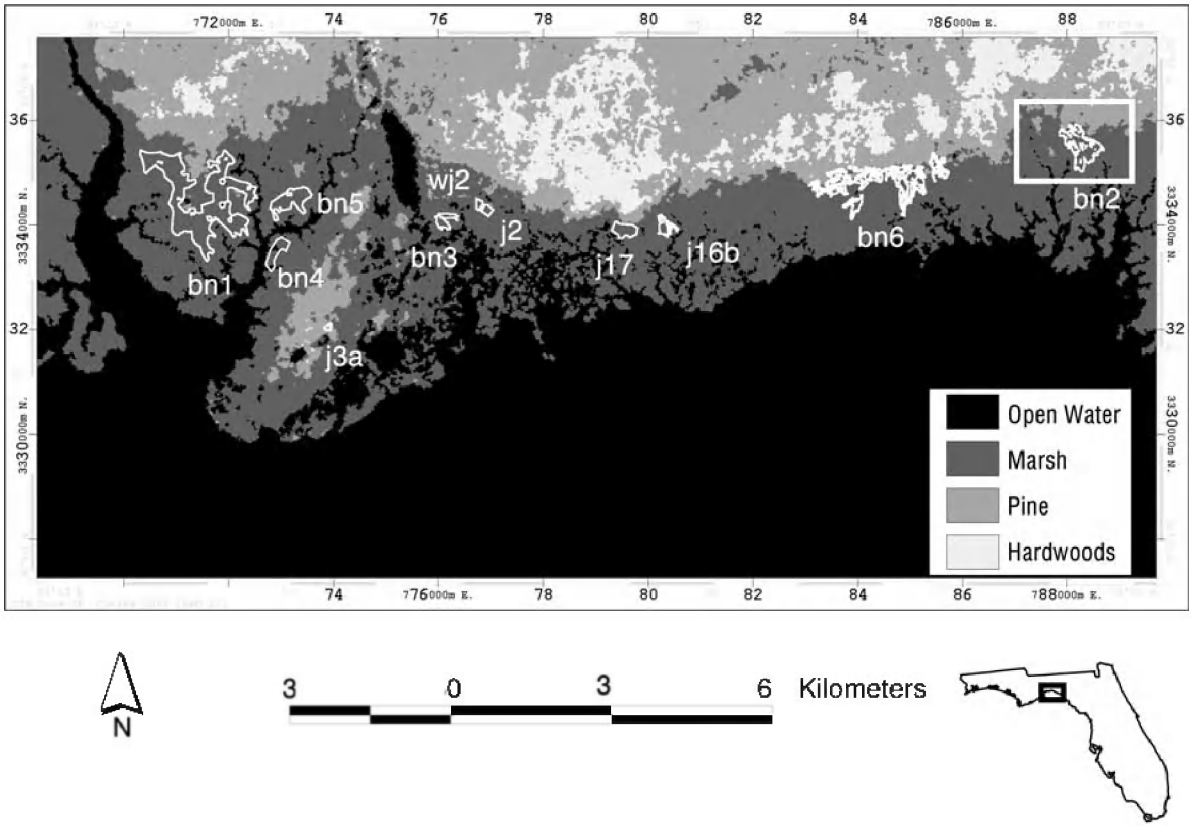

Figure 1. J. roemerianus coastal saline marsh sites within the St. Marks National Wildlife Refuge (NWR), Florida. The insert is illustrated in Figure 2.

Table 1. Study site, size (number of pixels and area), and burn date.

Site	No. of Pixels[a] (n)	Area (hectare)	Burn date
bn1[b]	1,606	100.4	06-Dec-85
bn1[b]	2,339	146.2	26-Feb-91
bn2	512	32.0	14-Mar-91
bn3	76	4.8	26-Dec-91
bn4	205	12.8	30-Dec-87
bn5	340	21.3	26-Feb-91
bn6	580	36.3	14-Mar-91
j2	60	3.8	28-Feb-90
j3a	28	1.8	08-Mar-92
j16b	135	8.4	05-Dec-91
j17	185	11.6	05-Dec-91
wj2	35	2.2	28-Feb-90

[a] 1 pixel = 25 m by 25 m spatial resolution.
[b] Site bn1 was burned twice.

Burn extents were identified on the 1988 and 1992 CIR photography (e.g., Figures 1 and 2; Table 1). Onscreen digitizing was used to produce 11 burn polygons (PCI Geomatics, 1998; Figure 1). Most burn extents included the high to medium high marsh area, but burn sites bn1 and bn6 extended into the low marsh areas (Ramsey et al., 1999). Two of the burn sites (j2 and j17) were located within impoundments (areas surrounded by levies that limit tidal flushing). For comparison, control areas near each burn that had not been burned within the last 3 years and occupied a similar marsh type as the burns were also identified. Difficulties arose where little to no nonburned marsh was left near the burn site (especially for the sites within the impoundments), and the complexity of the marsh terrain (e.g., channel dissection) precluded finding a control site that was expected to closely match the marsh type makeup of the burned marsh. In these cases, control areas were best estimates based on photography, site observations, and previous marsh classification (Ramsey et al., 1998, 1999). Digitized

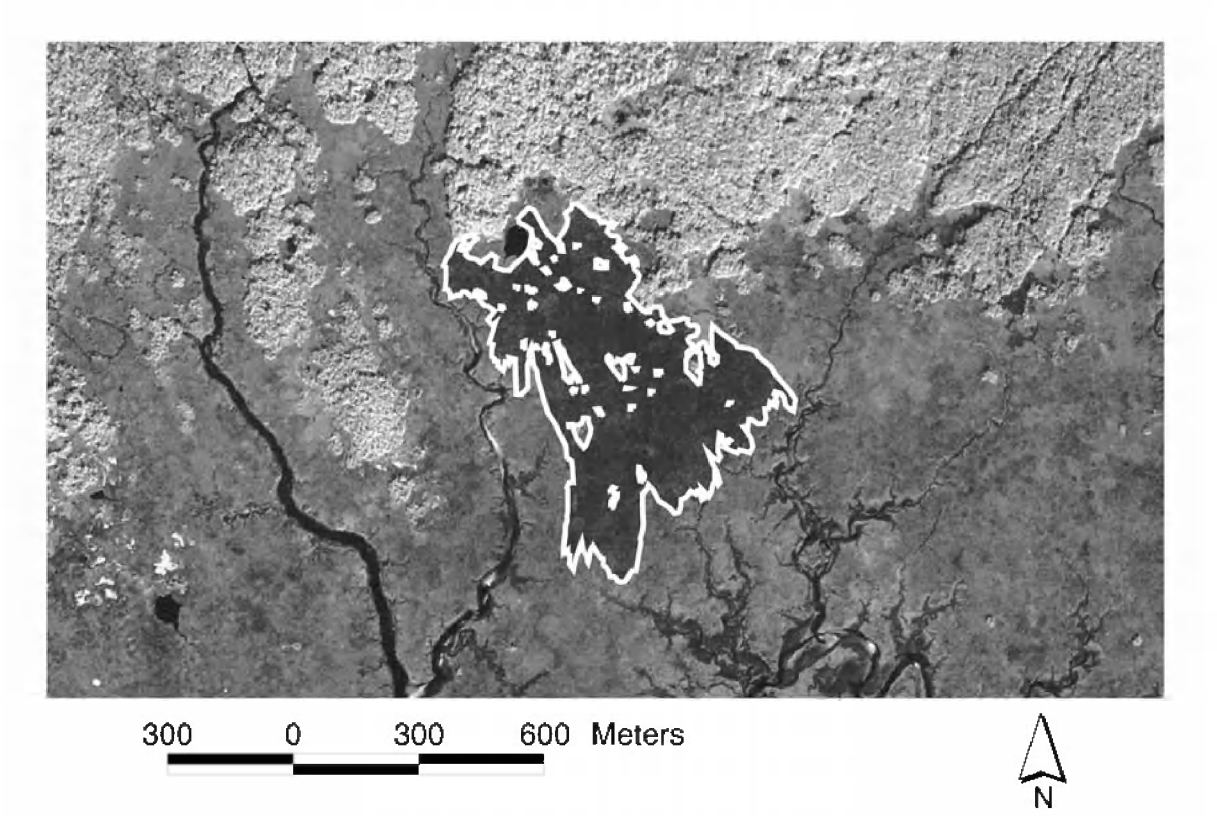

Figure 2. An example of how digitized polygons for the burn sites were defined in order to extract image data that occurred within each polygon.

polygons for both the burn and control sites were transformed into graphic masks and overlaid on each image (e.g., Figures 1 and 2). An overlay procedure was used to extract all image values that occurred within each polygon.

Subsequent to data extraction, the TM image data were transformed into a normalized difference vegetation index (NDVI) ([near infrared – red] / [near infrared + red]). NDVI has been extensively used and successfully related to indicators of vegetation biomass, especially green biomass (e.g., Sellers, 1987; Roughgarden et al., 1991; Ehrlich et al., 1994; Ramsey et al., 1997, 1998). Numerous studies have shown NDVI to be a robust and reliable estimator of vegetation trends and status (e.g., Eastman and Fulk, 1993; Samson, 1993; Andres et al., 1994; Ehrlich et al., 1994). However, NDVI may be sensitive to atmospheric conditions, view and sun zeniths, and background reflectances (Huete et al., 1985; Deering and Eck, 1987; Duggin and Robinove, 1990). In this study, we atmospherically corrected the TM data (Ahern et al., 1977; Ramsey and Jensen, 1990) before converting them to NDVI. Excluding influences related to background variability, these NDVI estimates more correctly indicate changes in *J. roemerianus* biomass, especially in the relative proportion of green biomass than NDVI estimates generated from non-atmospherically corrected image data. Subsequent to transforming the TM data to NDVI values, univariate statistics (e.g., mean, standard error) were generated for each polygon and each image (SAS, 1989). Assuming no correlation between burn and control sites, the standard error of the difference between burn and control sites NDVI's was estimated using the method of propagation of errors for unequal number of observations (Bevington, 1969) as

$$\sigma_{\overline{b-c}} = \sqrt{\frac{n_b\sigma_b^2 + n_c\sigma_c^2}{n_b + n_c}} \tag{1}$$

where, σ_b and σ_c are standard errors and n_b and n_c are number of observations from burn and control sites, respectively.

Burn dates were obtained from burn records compiled by the U.S. Fish and Wildlife Service at the St. Marks NWR (Table 1). Where discrepancies in the burn record existed, direct observations (e.g., CIR photography, field observation) were used to confirm or estimate the date of burn to within 2 to 4 months. At least four burn polygons incorporated marsh areas that had been burned more than once from early 1988 to late 1994. The most recent burn date was used for these burn polygons except for site bn1 where both burn dates were used; the second burn occurred within the current image collection dates. The time-since-burn was calculated as the difference between the date of the burn and the date of the image collection. Sites bn1 and bn4 were burned in December 1985 and 1987, respectively, up to 1,747 days before the closest TM collection. Sites j2 and wj2 were burned about 200 days prior to the earliest TM collection in September 1990. The rest of the sites were burned about 30 days after the February 1991 or about 60 to 90 days before the February 1992 TM image collections. Because of the limited samples, NDVI data related to burns occurring over 2,000 days earlier were excluded from the analysis.

Results

Linear fits to all points incorporating progressively longer time periods from the time of burn indicated increasingly lower rates of change in NDVI with increase in time-since-burn (Table 2). The highest rate of NDVI increase on average included data up to about 365 days since burn (7.5×10^{-4} ΔNDVI /Δdays). The lowest intercept was also associated with this time period (0.26 NDVI units). Even though NDVI should be near zero immediately following a burn, the regression estimates probably represent the best that can be obtained with a semiannual monitoring method.

Including all points (NDVI's) up to around 900 days after the burn indicated that NDVI tended to approach an average value of around 0.40 (Table 2). Using starting points ranging from 350 to 600 days since burn suggested that NDVI after reaching a mean high of around 0.52 to 0.57 tended to decrease at a rate between -1.2×10^{-4} and -1.7×10^{-4} ΔNDVI /Δdays (Table 2). According to the regression analysis, NDVI tended to increase sharply up to around 365 days from a potential low of about 0.26 and decrease slowly after reaching a potential high of around 0.52 to 0.57. Recovery seemed to take more than 900 days and approached a final NDVI around 0.40 (Table 2, Figure 3).

The regression analysis indicated the general trends to the burn recovery, and predicted extremes in the NDVI response that were slightly outside the range of the collected data. A 100-day moving average of the collected TM data also showed the general trend (Figure 3), but depicted subdued minimum and maximum responses. The subdued response most likely resulted from the inclusion of all available data representing variable offsets in the lapsed time from initial burn to the first TM collection date. Neither the regression nor the average analysis, however, could clarify if NDVI could be used to monitor individual burn site recovery over time. Site-specific burn and control mean NDVI's compared over time suggested a general progression similar to the more general regression results (Figure 4): a high increase and then decrease following burn. In addition, the comparison suggested that from the time of burn to possibly 6 months later, burn NDVI's were lower than control (nonburn) NDVI's. For around another year after this initial recovery, the NDVI's associated with burns overshot the NDVI's associated with control sites. After these recovery phases, the burn and control NDVI's often converged (Figures 3 and 4).

Comparison of the control and burn sites revealed a slight tendency for a higher and then lower NDVI in the winter and then summer, respectively, especially in the preburn NDVI's. Added to this, most of the marsh burns occurred during the winter months and TM collections were in both the winter and summer. In essence, the possible winter and summer increase and decrease in marsh NDVI coincided with the TM collections. To remove the possible seasonal variation, the mean NDVI's generated for the controls were subtracted from the mean NDVI's of the respective burn site (e.g., mean NDVI of (bn1 burn site – bn1 control site)) (Figure 5).

The subtraction also lessened other canopy alterations not related to burn recovery. Four major storms impacted the marsh during the 4 years of TM collections (e.g., Figure 4): Hurricane Andrew of 22–26 August 1992, the superstorm of 13 March 1993 occurring 5 days before the TM collection, the unnamed flooding event of 5 March 1994 peaking on the day of the TM collection, and Tropical Storm (TS) Beryl occurring a month before the 13 September 1994 TM collection date.

Four main consequences of these storm impacts to applying NDVI following burn impact and recovery

Table 2. Regression analysis of the time-since-burn and mean NDVI obtained from various burn sites.

Time-since-burn (days)	Number of Observations (n)	Intercept (NDVI Magnitude)	Slope (NDVI/Day) $\times 10^{-4}$	R^2	p-value
0 to 365	18	0.26	7.5	0.60	0.0001
0 to 450	23	0.28	6.1	0.56	0.0001
0 to 550	33	0.35	2.5	0.23	0.0047
0 to 700	36	0.36	2.3	0.24	0.0022
0 to 800	44	0.39	1.2	0.12	0.0208
0 to 900	51	0.40	0.8	0.07	0.0544
350 to 1150	50	0.53	–1.3	0.23	0.0004
500 to 1150	41	0.52	–1.2	0.14	0.0142
600 to 1150	33	0.57	–1.7	0.20	0.0093

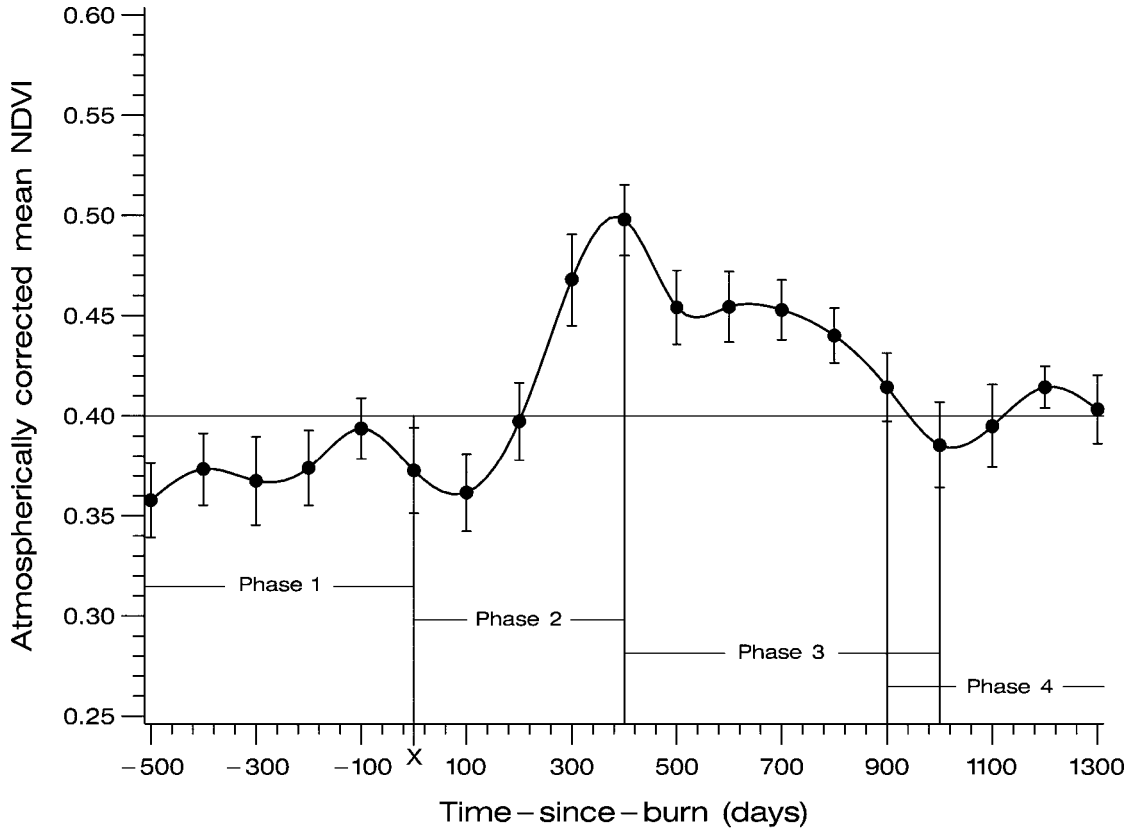

Figure 3. A generalized depiction of the progression of marsh NDVI following an intense burn. The combined data associated with the 11 burn sites were used to generate the means and standard errors shown. Note that 'X' on the abscissa indicates the burn date. Also, notice that the highest rate of NDVI increase occurs within about 365 days following the burn after which time it asymptotes to a NDVI typifying a mature *J. roemerianus* marsh.

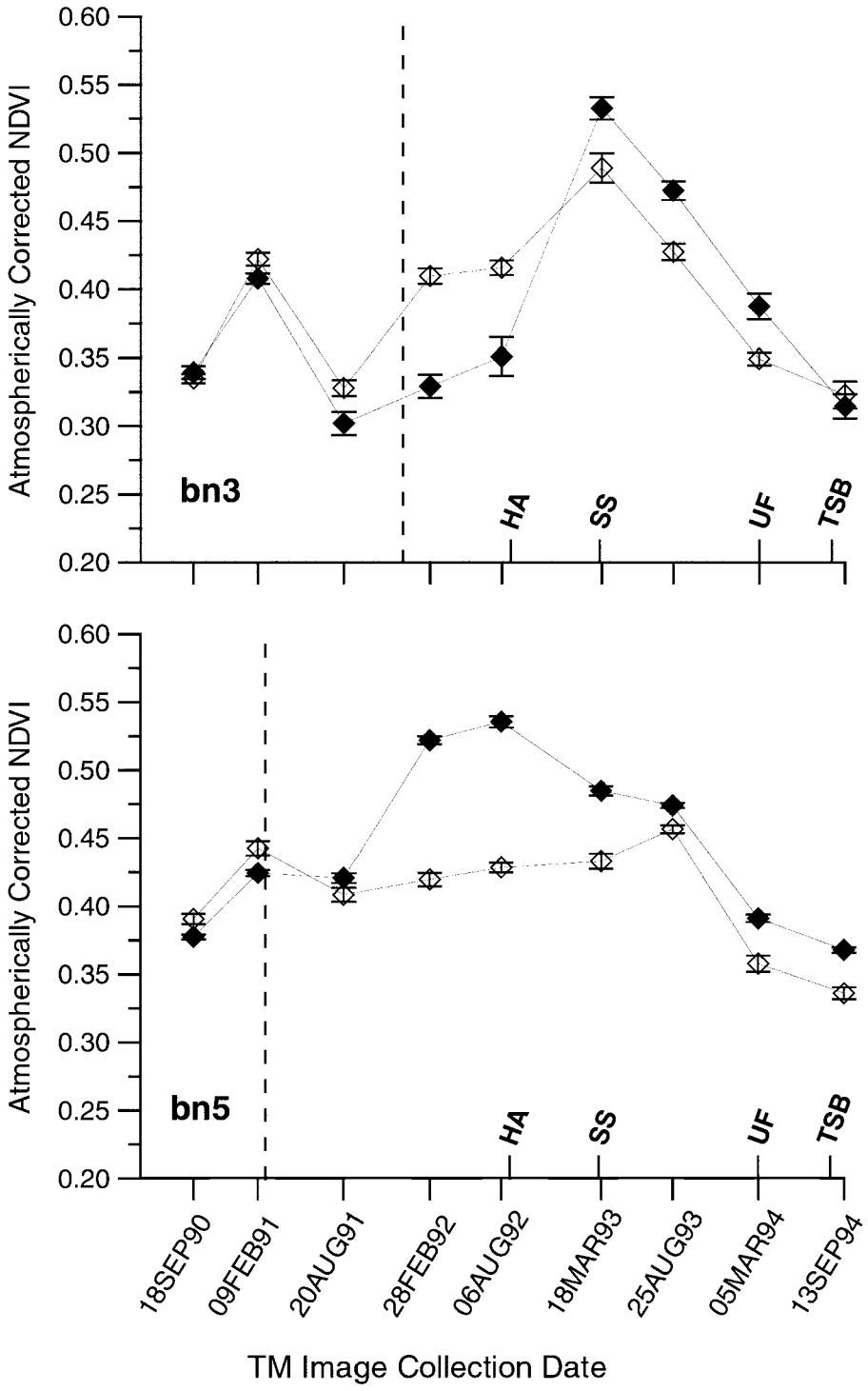

Figure 4. Examples of site-specific burn (solid symbol) and control (open symbol) mean NDVI's compared over time. Note the depressed and subsequently elevated burn NDVI compared to the control (unburned) NDVI's following a burn. Also note the times of storm occurrences (HA – Hurricane Andrew, SS – Superstorm, UF – Unnamed Flood, TSB – Tropical Storm Beryl). Vertical dashed lines indicate the time of burn. Standard errors, graphically shown as error bars, were calculated from the atmospherically corrected NDVI values generated per pixel per burn and control sites for each image date.

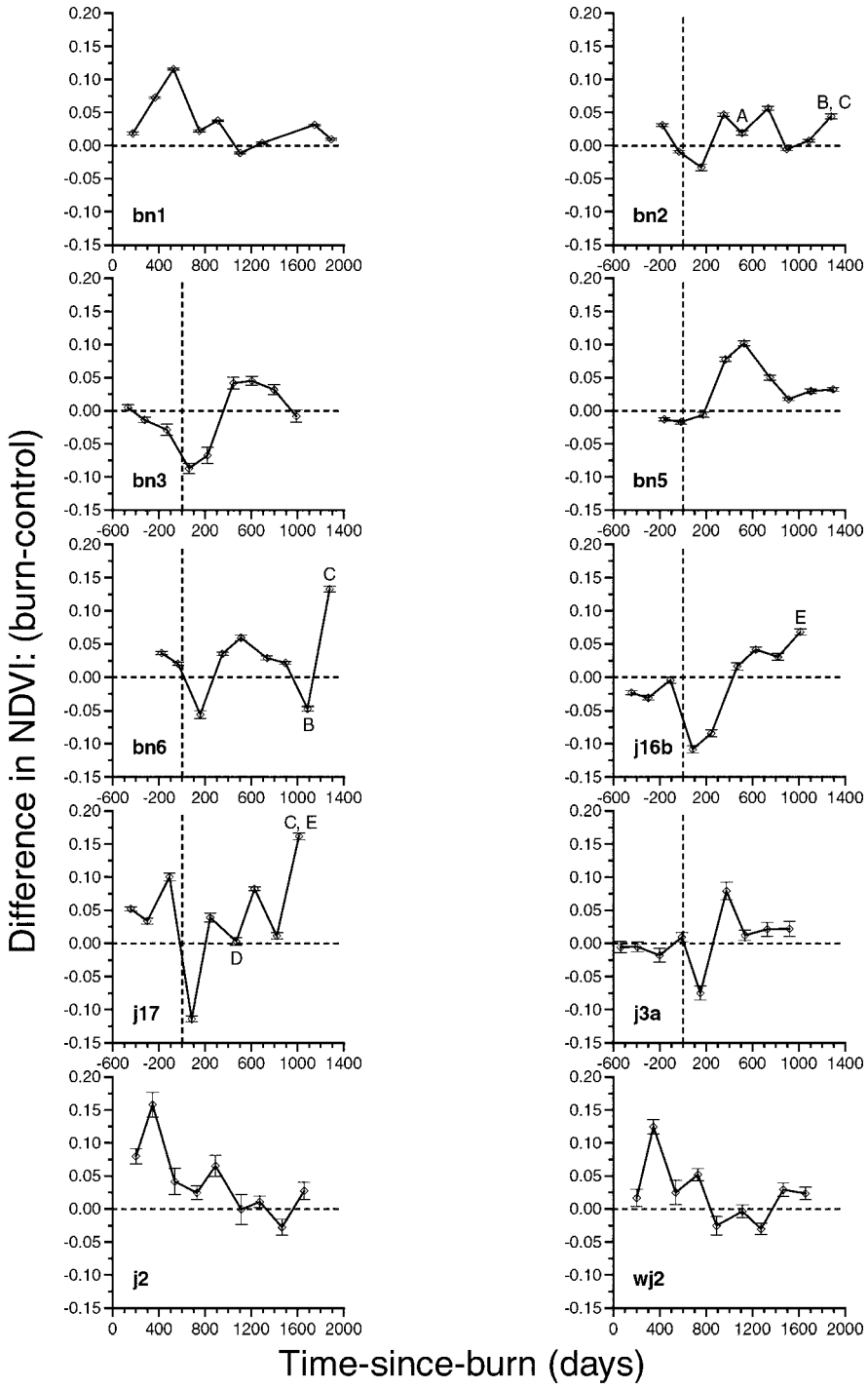

Figure 5. The result of subtracting the mean NDVI's generated for the controls from the mean NDVI's of the respective burn site. Note the variation in offsets between the time of burn and the time of the first image collection. Also note the upper case letters indicating abnormalities in the burn trends. 'A' indicates possible cloud influences, 'B' secondary burn influences, 'C' abnormal green growth, 'D' dead materials on burn site, and 'E' dead materials on control site. Standard errors, graphically shown as error bars, were calculated using Equation 1.

trends were noted in our field occupation and visual analysis of the image data. First, major flooding submerging a large portion of the plant canopy at the time of the TM collection diminished NDVI. Second, storms at times deposited large areas of dead grasses in seemingly random locations throughout the high saline marsh. Third, the saline marsh was swept partly to totally clean of dead material. Fourth, heavy rainfall sometimes following the inland track of the storm resulted in prolonged flushing of the impounded saline marshes with fresh water.

The 1994 unnamed flood event created high water in the marsh at the time of the TM data collection, diminishing burn and control site NDVI's nearly equally (e.g., Figures 4). In this case, subtraction minimized the flooding effects on NDVI. The 1993 superstorm and 1994 TS Beryl deposited large amounts of dead materials in the upper marsh areas. Rainfall resulting from the unnamed flood and TS Beryl caused a deluge of freshwater runoff and flooding. We expect concurrent flooding and dead material deposits to diminish NDVI, but expect prolonged freshwater flooding that excludes regular saline flushing to increase NDVI.

Abnormality in the burn record of bn2 site possibly resulted from residual cloud influences in the 6 August 1992 image and the storm deposits in the 18 March 1993 possibly diminished NDVI values of burn site site j17. Broadly, however, sites physically nearby, and burned close to the same date, were associated with similar shape and magnitude difference plots (Figure 5, e.g., bn6 and bn2, bn3 and j16b, and j2 and wj2). Shape and magnitude differences between sites not burned at the same time could be partly a result of differences between the time of the burn and the image collections. NDVI's generated from images collected almost immediately following the burn date would likely be lower than those collected further from the burn date.

Besides similarities of burns close in space and time, bn5 follows the general shape portrayed at sites bn6 and bn2, as does j17 after accounting for the plausible NDVI decrease caused by the superstorm deposit of dead materials. Further, the recovery trend associated with bn1 is comparable to trends at j2 and wj2. The trend at site j3a, however, differs noticeably from all other sites. Possibly this difference results from j3a being associated with the lowest offset time between TM collect and burn times, or from j3a being the smallest site, and therefore, the most prone to signal contamination by the surrounding marsh. Even though somewhat different trends emerged in this analysis, all sites, including j3a, reveal a broadly similar pattern in burn recovery. Initial recovery (Phase 2) lasted about 300 to 500 days, and excluding site j3a, Phase 3 about 500 to 600 days. Total recovery time lasted about 900 to 1,000 days after burn. Finally, the difference trend associated with site bn4 burned nearly three years before the first TM collection hints that a slight difference in NDVI may exist for up to 1,300 days after the burn. The lack of supporting data, however, restricted the use of this site in the analysis.

Another noticeable inconsistency in the conjectured four phase burn cycle was seen in sites j2, bn2, j16b, bn6, and j17. The inconsistency concerns an abnormally high 13 September 1994 NDVI, especially at sites bn2 and bn6. Site bn2 was partially and bn6 totally burned in December 1993 just before the 5 March 1994 TM collection. The partial bn2 burn was associated with a the slight increase in NDVI whereas the total burn of site bn6 was associated with a dramatic increase in NDVI from after the burn until the last TM collection. Abnormally high NDVI's at sites j16b and j17 may be related to another event causing marsh alteration. Large amounts of dead materials were deposited at a number of higher marsh locations during TS Beryl about 1 month before the September 1994 TM collection. There was no discernable pattern to where these deposits were located other than associated with more high marsh to transition areas. The control site for j16b and j17 was heavily impacted by the deposited dead materials, resulting in a relatively lower NDVI control. Consequently, the lower NDVI control resulted in a positive increase in the j16b and j17 NDVI differences.

The burn and control NDVI difference associated with site j17 was much higher than for site j16b causing suspicion that there was an additional cause for the elevated j17 NDVI difference. Another effect of the TS Beryl impact was deluge of rainfall as the storm traveled inland. For a good part of the month before the September 1994 TM collection, fresh water flooded the inland areas but only flooded the marsh for a few days. Site j17, in contrast to site j16b and their common control, lies within an impoundment at the farthest landward extent of the saline marsh. During the fresh water flood onslaught, the leaky levee system maintaining the impoundment could be expected to be influenced mostly, if not totally by freshwater, excluding the impacts of saline flushing. This exclusion of saltwater flushing may have lessened the stress on the *J. roemerianus* marsh resulting in a biomass in-

crease (Eleuterius, 1989), and thus, a sudden increase in NDVI.

Discussion and conclusion

In the process of examining the relationship between NDVI and time-since-burn, we uncovered a pattern in the burn recovery of *J. roemerianus*. Grouping the burn sites data together according to the time-since-burn, the rate of change of NDVI progressively decreased and the intercept steadily increased with addition of longer time spans since burn date. On average there was about a 0.26 to 0.31 change (intercept) in NDVI from a low of about 0.26 immediately after the burn to a high of about 0.52 to 0.57 following the burn. The high initial burn recovery rate (slope) of about 7.5×10^{-4} ΔNDVI/Δdays resulted in an initial average recovery duration of about 340 to 400 days. During this phase of increasing NDVI, the ability to predict the time-since-burn was within about $\pm$60 days (prediction error). After this initial period, NDVI associated with recovering burns decreased at a rate between about -1.2 and -1.7×10^{-4} ΔNDVI/Δdays. Dividing the change in NDVI from its maximum magnitude (0.52 to 0.57) to its final value around 0.40 by the rate of decrease resulted in an estimated total time to recovery of about 1000 days. During this phase of decreasing NDVI, the inverse regression showed the ability to predict the time-since-burn was within about $\pm$88 days.

Closer inspection of the burn and image collection dates, however, indicated that changes in NDVI were not only related to burn recovery, but also to seasonal changes, storm impacts, and variable offsets between the time of burn to the first image collection. NDVI trends adjusted to the time-since-burn did alleviate most of the burn comparisons difficulties; however, the time offset between the burn occurrence and the first subsequent image collection could not be adjusted. Offset variability seemed to cause differences in the magnitude of initial decrease and subsequent increase in NDVI. Sites physically close or burned at about the same time had similar NDVI trends; however, the offset influence was not predictable and resulted in some variation in shape and magnitude of the post burn NDVI trends. Burn recovery at most sites, however, could broadly be described to have similar trends.

Tendencies for additional nonburn-related influences to alter the NDVI trend were also revealed. Possible seasonal dependencies and differential storm responses seemed to be the most likely causes of the nonburn related changes. Seasonal variation was slight, but it seemed to indicate a pattern of somewhat higher NDVI's in the late winter than in the late summer. This pattern is reflected in live and dead biomass measurements at one *J. roemerianus* site reported by Hopkinson et al. (1978). At this site, live biomass peaked between February and June while dead biomass peaked from June to September. Subtraction of the control sites NDVI from the burn sites NDVI eliminated most of the nonburn related influences but slight influences remained. The remaining influences appeared to be related to either storm impacts or secondary burning. Storm impacts included dead material deposits, flood occurrence during the image collection, and enhanced freshwater runoff. These influences were not spatially uniform resulting in differential responses at the site scale. Secondary burning, including part or all of the burn sites, also altered the burn recovery sequence. The magnitude of alteration depended on the percent of the site burned and on the time offset between the burn and image collection dates.

In this study, we demonstrated that when properly corrected for atmospheric influences, changes in TM data transformed into NDVI could be related to burn recovery in a *J. roemerianus* coastal marsh. Standardizing the time-since-burn minimized variability related to the time of the burn occurrence; however, variability remained related to differences in the length of time between burn and TM collection. Controls were needed to diminish broad scale influences (e.g., seasonal changes, coastal flooding) and collateral sources (e.g., site photography and flood records) of the study area, in general, were necessary to relate secondary burns and storm impacts to remaining abnormalities in the burn recovery sequence. Accounting for these influences and abnormalities allowed the recovery trends to be standardized into four general phases: Phase 1 – preburn, Phase 2 – initial recovery (increasing NDVI), Phase 3 – late recovery (decreasing NDVI), and Phase 4 – final coalescence (unchanging NDVI). As found in the regression analysis, Phase 2 tended to last on an average of 300 to 500 days. Phase 3 lasted an additional 500 to 600 days, but was 300 to 400 days at one site. In most cases, Phase 4 was reached within 900 to 1,000 days after the burn.

The relationship between NDVI and time-since-burn indicates that NDVI is a relatively inexpensive and useful tool for monitoring the recovery of a burned *J. roemerianus* coastal marsh and perhaps for monitoring the recovery of similar marshes with severe

impacts (e.g., due to fire, storm, herbivory, oil spill). These results confirm suggestions provided in previous studies that *J. roemerianus* marshes recover slowly from acute impacts (Hopkinson et al., 1978; Ramsey et al., 1992, 1999). Results also suggest a tendency for the relative amount of live biomass, positively associated with NDVI, to be slightly higher in the winter than summer. Any seasonal trends, however, can be obscured by secondary burns and storm impacts. If a method were available for eliminating or explaining local differences detection of abnormalities in the standardized NDVI trends could allow operational detection of severe impacts to the marsh and the assessment of the recovery progression. The same technique might be used to detect and monitor other types of severe impacts, such as from herbivory and storms. Standardized NDVI trends might also allow the analysis of more subtle variations, such as seasonal variability and degradation of the marsh due to alteration of the hydrologic or salinity regime. Finally, to increase data collection frequency, we are exploring the use of alternate remote sensing systems (e.g., active and passive microwaves) that are not affected by clouds or darkness (e.g., Ramsey, 1998; Ramsey et al., 1998, 1999). These new data sources may supplement the NDVI information, and thus, improve the ability to consistently and timely monitor the status and trends of these coastal resources.

Acknowledgements

We thank James Burnett and Joe White of the U. S. Fish and Wildlife Service for access to the St. Marks National Wildlife Refuge, Florida, and John Fort and Doug Scott for help in field logistics and data collections. We are grateful to U.S. Geological Survey personnel Richard Day, Scott Wilson, and Kevin McRae for the many hours of work on this study. We thank Dr Sammy King of U.S. Geological Survey for reviewing the earlier version of the manuscript. We also thank Ms Beth Vairin for editing this manuscript.

References

Ahern, F.J., Goodenough, D.G., Jain, S.C. and Rao, V.R. 1977. Use of Clear Lakes as Standard Reflectors for Atmospheric Measurements. Proceedings, Eleventh International Symposium on Remote Sensing of Environment on 25–29 April 1977 (Ann Arbor: Environmental Institute of Michigan), pp. 731–755.

Andres, L., Salas, W.A. and Skole, D. 1994. Fourier analysis of multitemporal AVHRR data applied to a land cover classification. Int. J. Remote Sens. 15(5): 1115–1121.

Bevington, P.R. 1969. Data Reduction and Error Analysis for the Physical Sciences. McGraw-Hill, Inc., New York, 336 pp.

Deering, D.W. and Eck, T.F. 1987. Atmospheric optical depth effects on angular anisotropy of plant canopy reflectance. Int. J. Remote Sens. 8(6): 893–916.

Duggin, M.J. and Robinove, C.J. 1990. Assumptions implicit in remote sensing data acquisitions and analysis. Int. J. Remote Sens. 11(10): 1669–1694.

Eastman, J.R. and Fulk, M. 1993. Long sequence time series evaluation using standardized principal components. Photogram. Eng. Remote Sens. 59(8): 1307–1312.

Ehrlich, D., Estes, J.E. and Singh, A. 1994. Applications of NOAA-AVHRR 1 km data for environmental monitoring. Int. J. Remote Sens. 15(1): 145–161.

Eleuterius, L.N. 1989. Natural selection and genetic adaptation to hypersalinity in *Juncus roemerianus* Scheele. Aq. Bot. 36: 45–53.

Hopkinson, C.S., Gosselink, J. and Parrondo, R.T. 1978. Aboveground production of seven marsh plant species in coastal Louisiana. Ecology 59: 760–769.

Huete, A.R., Jackson, R.D. and Post, D.F. 1985. Spectral response of a plant canopy with different soil backgrounds. Remote Sens. Env. 17: 37–53.

Johnson, S. and Knapp, A. 1993. The effect of fire on gas exchange and aboveground biomass production in annually vs. biennially burned *Spartina pectinate.* Wetlands 13: 299–303.

Kruczynski, W.L., Subrahmanyam, C.B. and Drake, S.H. 1978. Studies on the plant community of a North Florida salt marsh, part 1, primary production. Bull. Marine Sci. 28(2): 316–334.

Lulla, K. and Mausel, P. 1983. Ecological applications of remotely sensed multispectral data. *In:* Richasen, B.F., Jr. (ed.), Remote Sensing of the Environment. pp. 354–377. Hunt, Dubuque, Iowa.

PCI Geomatics, 1998. Using PCI Software, Version 6.3 EASI/PACE. PCI Geomatics, Richmond Hill, Ontario, Canada.

Ramsey III, E.W. and Jensen, J.R. 1990. The derivation of water volume reflectances from airborne MSS data using *in situ* water volume reflectances, and combined optimization technique and radiative transfer model. Int. J. Remote Sens. 11(6): 979–998.

Ramsey III, E.W, Chappell, D.K. and Baldwin, D. 1997. AVHRR imagery used to identify Hurricane Andrew damage in a forested wetland of Louisiana. Photogram. Eng. Remote Sens. 63: 293–297.

Ramsey III, E.W. 1998. Radar remote sensing of wetlands. *In*: Lunetta, R. and Elvidge, C. (eds.), Remote Sensing Change Detection: Environmental Monitoring Methods and Applications, pp. 211–243. Ann Arbor Press, Chelsea, Michigan.

Ramsey III, E.W., Nelson, G.A. and Sapkota, S.K. 1998. Classifying coastal resources by integrating optical and radar imagery and color infrared photography. Mang. Salt Marsh. 2: 109–119.

Ramsey III, E.W, Nelson, G.A, Sapkota, S.K, Laine, S.C, Verdi, J. and Krasznay, S. 1999. Using multiple-polarization L-band radar to monitor marsh burn recovery. IEEE Trans. Geosci. Remote Sens. 37: 635–639.

Ramsey III, E.W, Spell, R. and Day, R.M. 1992. Light Attenuation and Canopy Reflectance as Discriminators of Gulf Coast Wetland Types. Proceedings of the International Symposium on Spectral Sensing Research Vol. II held in Maui, Hawaii on 15–20 November.

Roughgarden, J., Running, S.W. and Matson, P.A. 1991. What does remote sensing do for ecology? Ecology 72(6): 1918–1922.

Samson, S.A. 1993. Two indices to characterize temporal patterns in the spectra response of vegetation. Photogram. Eng. Remote Sens. 59: 511–517.

SAS Institute Inc. 1989. SAS/STAT User's Guide, version 6, 4th ed., vol. 2, Cary, NC, 846 pp.

Sellers, P.J. 1987. Canopy reflectance, photosynthesis, and transpiration. Part II. The role of biophysics in the linearity of their interdependence. Remote Sens. Environ. 21: 143–183.

Stout, J. 1984. The Ecology of Irregularly Flooded Salt Marshes of the Northeastern Gulf of Mexico: A Community Profile. U.S. Fish & Wildlife Service Biological Report 85 (7.1): 98 pp.

Taylor, K., Grace, J., Guntenspergen, G. and Foote, A.L. 1994. The interactive effects of herbivory and fire on an oligohaline marsh, Little Lake, Louisiana, USA. Wetlands 14: 82–87.

Teuber, K.B. 1990. Use of AVHRR imagery for large-scale forest inventories. Forest Ecol. Manag. 33/34: 621–631.

Williams, R. and Murdoch, M. 1972. Compartmental analysis of the production of *Juncus roemerianus* in a North Carolina salt marsh. Chesapeake Sci. 13: 69–79.